Journal of Non-Crystalline Solids 355 (2009) 2485–2490

Contents lists available at ScienceDirect

Journal of Non-Crystalline Solids

journal homepage: www.elsevier.com/locate/jnoncrysol

Evaluation of basic physical parameters of quaternary Ge–Sb-(S,Te) chalcogenide glasses

V. Pamukchieva [a,*], A. Szekeres [a], K. Todorova [a], M. Fabian [b], E. Svab [b], Zs. Revay [c], L. Szentmiklosi [c]

[a] Institute of Solid State Physics, Bulgarian Academy of Sciences, Tzarigradsko Chaussee 72, 1784 Sofia, Bulgaria
[b] Research Institute for Solid State Physics and Optics, Konkoly Thege str. 29-33, H-1525 Budapest, P.O. Box 49, Hungary
[c] Institute of Isotopes, Konkoly Thege str. 29-33, H-1525 Budapest, P.O. Box 49, Hungary

ARTICLE INFO

Article history:
Received 10 November 2008
Received in revised form 9 July 2009
Available online 24 September 2009

PACS:
61.43.Fs
61.43.–j

Keywords:
Amorphous semiconductors
Neutron diffraction/scattering
Chalcogenides
Monte-Carlo simulations

ABSTRACT

New quaternary chalcogenide $Ge_xSb_{40-x}S_{50}Te_{10}$ (x = 10, 20 and 27 at.%) and $Ge_xSb_{40-x}S_{55}Te_5$ (x = 20 and 27 at.%) glasses have been synthesized and the compositions have been characterized applying prompt gamma-ray activation analyses, neutron diffraction, and material density measurements. Using the experimental data, the basic physical parameters, such as average atomic volume, packing density, compactness, average coordination number, number of constrains, average heat of atomization and cohesive energy, of the synthesized glasses are evaluated and the results are discussed in a function of glass composition.

1. Introduction

Chalcogenide glasses have unique properties for potential application in the field of infrared optics, fiber optics, memory devices, inorganics photoresists, and antireflection coatings [1–6]. These glasses are low phonon energy materials, and are transparent for light in the visible and mid-infrared region. The position of the infrared multi-phonon absorption edge follows the Szigeti relationship [7], thus glasses with heavier atoms and weaker atomic bonding transmit light to longer wavelengths. For example, in the short optical pathlengths of micron-scale the sulphide based glasses, such as As_2S_3, have a transparent window from the mid-visible (~500 nm) to ~8 μm. Also, selenide glasses, such as Ge–As–Se based compositions, have transparent windows from ~0.7 to ~14 μm, while quaternary Ge–As–Se–Te compositions have also a wide range of transparency from ~2 μm up to ~20 μm. They show continuous change of physical properties with the chemical composition.

It is well known that Te atom is much heavier than S atom and the introduction of small amount of Te into the glass leads to stabilization of the glass structure and to a reduction of the phonon energies [8]. Due to the transparency in the infrared spectral region and the high refractive index and photosensitivity, telluride glasses from quaternary systems are potential candidates for integrated optics. In recent years the number of papers dealing with such telluride glasses has increased [9–16], which reflects the growing interest in these materials. Still, there is no comprehensive study of the influence of Te substitution for S on the structure and properties of the glasses belonging to the quaternary Ge–Sb–S–Te system.

Another aspect in the studies of Ge–Sb–S–Te alloys is the proximity of Sb and Te in the periodic table, which is the reason for Te and Sb to resemble each other. One has to be very careful in modelling because the small difference between Sb and Te sometimes cannot be distinguished. This problem represents still another reason to perform a systematic study across a family of alloys and to avoid basing conclusions on distinguishing between these atoms. Moreover, Te based glasses could be very interesting for the production of optics devices for the far infrared, thanks to their low phonon character due to the high atomic weight of Te.

In this paper we present results on the evaluation of some physical properties of a new quaternary telluride system, synthesized by us, based on Ge–S glasses with addition of Sb and partial substitution of Te for S. The basic parameters, namely material density, packing density, average atomic volume, compactness, coordination number, number of constrains, cohesive energy, and heat of atomization in dependence on glass composition, are considered.

* Corresponding author.
E-mail address: vesela@issp.bas.bg (V. Pamukchieva).

0022-3093/$ - see front matter © 2009 Elsevier B.V. All rights reserved.
doi:10.1016/j.jnoncrysol.2009.08.028

Calculations of these parameters are made on the basis of the density and composition measurements on these glasses. Knowing the values of the glass density, average atomic volume, and coordination number one can predict the glass transition temperature and the optical band gap of the glasses applying the Tichy–Ticha approach [17,18]. The average heat of atomization is related to the photon energy [19], at which the optical absorption coefficient of the material is 10^4 cm^{-1} and, therefore, it correlates with the optical bandgap energy of the material.

2. Experimental

2.1. Glass synthesis and density measurement

The bulk glasses with composition of $Ge_xSb_{40-x}S_{50}Te_{10}$ (x = 10, 20 and 27 at.%) and $Ge_xSb_{40-x}S_{55}Te_5$ (x = 20 and 27 at.%) were synthesized from 5 N purity elements by the conventional melt-quenching method. The synthesis was performed in a rotary furnace, as the glass components of a proper composition were placed in quartz ampoules, which was evacuated (10^{-3} Pa). The ampoules were heated up to 950 °C with a rate of 2.5 °C/min and were kept at this temperature for 24 h, rotating the furnace for homogeneous melting. Ending the process, the ampoules were pulled out and sharply dropped to room temperature, quenching in air. Finally, the bulk glasses were taken from the ampoules.

The density of the synthesized materials, ρ, was measured by applying Archimedes method using the hydrostatic weighing in toluene. For each composition the measurement was repeated four times and the obtained ρ values were averaged. The ρ values are determined with an accuracy of ±0.01 g/cm^3 from the relation,

$$\rho = \rho_{tol} W_{air}/(W_{air} - W_{tol}), \quad (1)$$

where W_{air} and W_{tol} are the weight of the sample in air and in toluene, respectively. The averaged density for each composition is given in Table 1. The material density decreases with increasing the Ge content or with decreasing the Te content.

2.2. Measurements of composition and structure of the synthesized glasses

Information about the composition of the glasses and their structure was obtained from the prompt gamma-ray activation analyses (PGAA) and the neutron diffraction (ND) measurements at the 10 MW Budapest Research Reactor. The ND measurements were performed on a 'PSD' neutron diffractometer with a monochromatic wavelength of λ_0 = 1.068 Å [20]. The diffraction spectrum of the powdered material was measured in a momentum transfer range of Q = 0.45–9.8 Å^{-1}. Each powdered glass with a weight of about 2–3 g was put in a cylindrical vanadium sample holder of 8 mm diameter, 50 mm height and 0.07 mm wall thickness. The correction and normalization procedures utilized to obtain the total structure factor $S(Q)$ from the measured pattern are described in our previous work [21].

By analysing the PGAA data, the Ge, Sb, Te, and S components of the glasses were determined with relative uncertainties being within 2–3%. The obtained results are summarized in Table 1. As is seen, the glass compositions are well-correlated with those preliminary calculated for the glass synthesis.

From the neutron diffraction measurements of the Ge–Sb–S–Te specimens the experimental spectra of the total structure factor $S(Q)$ were derived. The results are presented in Fig. 1. The peaks are broad and with a wavy character being typical for an amorphous material. In each curve the peaks are situated around 1.1, 2.1, 3.6, 5.6, 7.4 and 9.0 Å^{-1} along the Q axis. With increasing the Ge content, the intensity of the first peak increases, whereas the second peak broadens and its intensity decreases.

Further, we applied direct Fourier transformation (FT) for the $S(Q)$ data analysis to calculate the reduced distribution function, $G(r)$, as:

$$G(r) = \frac{2}{\pi}\int_o^{Q_{max}} Q[S(Q) - 1]\sin Qr\ dQ. \quad (2)$$

Fig. 2 shows the $G(r)$ functions calculated from the $S(Q)$ data using Eq. (2). Due to the relatively low value of Q_{max} = 9.8 Å^{-1} in the present experiment, the r-space resolution is rather low, $\Delta r = \frac{2\pi}{Q_{max}} \approx 0.6$ Å, therefore the partial atomic pair distances are not resolved, as they overlap in the detected broad peaks. The main peaks appear around 2.3, 3.6, 4.4 and 5.4 Å and they correspond to the 1st, 2nd and 3rd coordination spheres, as it is indicated by arrows in Fig. 2.

The total atomic pair correlation function, $g(r)$, which characterizes the one-dimensional average atomic pair correlation, was calculated from the simulation of the experimental $S(Q)$ data by applying the Monte-Carlo method with MCGR program [22]. The MCGR method is a one-dimensional version of the reverse Monte-Carlo (RMC) modelling [23]. The relation between $G(r)$ and $g(r)$ functions are expressed as:

$$G(r) = 4\pi\rho r[g(r) - 1], \quad (3)$$

where ρ is the measured glass density presented in Table 1. The simulation procedure allows for atomic movements in order to minimize the difference between model and experimental $S(Q)$ values. The starting model for atomic configuration in the MCGR simulation was built up with a box containing 10 000 atoms and with a half-box length of 35.5 Å, the atoms having a completely random distribution. We used a cut-off constraint of 1.1 Å for each atomic pair and no further constraints were considered. From Fig. 1 it is well seen that the MCGR simulation curves (solid line) describe well the experimental data (empty circles).

Fig. 3 shows the $g_{MCGR}(r)$ functions for three Ge–Sb–S–Te glass compositions. The coordination spheres are indicated by arrows using a similar system of notation as introduced in Fig. 2. In the 1st coordination sphere two distinct peaks appear at ~2.3 and ~2.8 Å, which can be related to the Ge–S and Sb–Te first neighbour distances, respectively [24–26]. The Ge–Ge first neighbour distance is expected around 2.4 Å [25,26] but it

Table 1
Composition of Ge–Sb–S–Te glasses for synthesis, composition of the synthesized Ge–Sb–S–Te glasses and their density, (ρ).

Composition of Ge–Sb–S–Te glasses for synthesis (at.%)				Measured ρ (g/cm^3)	Composition of synthesized Ge–Sb–S–Te glasses, measured by PGAA (at.%)			
Ge	Sb	S	Te		Ge	Sb	S	Te
10	30	50	10	4.29 ± 0.01	9.4 ± 0.3	29.7 ± 0.6	50.2 ± 0.8	10.7 ± 0.2
20	20	50	10	3.95 ± 0.01	19.4 ± 0.5	19.5 ± 0.5	50.6 ± 0.8	10.4 ± 0.2
27	13	50	10	3.74 ± 0.01	25.4 ± 0.7	13.3 ± 0.4	51.1 ± 0.8	10.2 ± 0.2
20	20	55	5	3.76 ± 0.01	19.2 ± 0.5	19.3 ± 0.5	56.1 ± 0.8	5.4 ± 0.1
27	13	55	5	3.54 ± 0.01	25.2 ± 0.7	13.1 ± 0.4	56.4 ± 0.8	5.3 ± 0.1

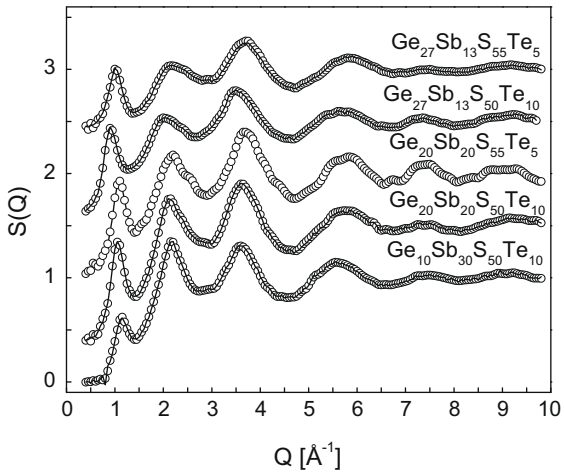

Fig. 1. Compositional dependence of the neutron diffraction structural factor $S(Q)$: measured data (circles) and data calculated by the MCGR simulation method (solid line) for the studied Ge–Sb–S–Te glasses. The curves are shifted vertically for clarity.

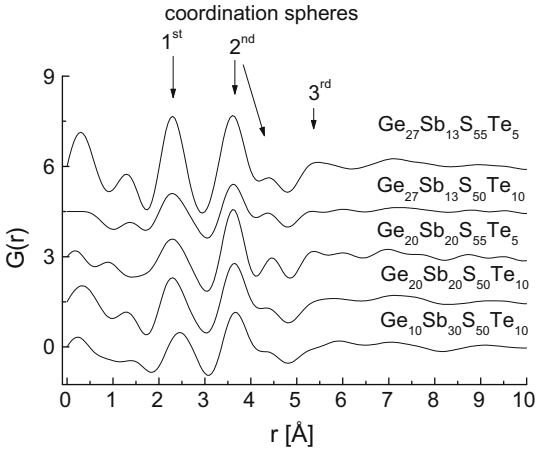

Fig. 2. Reduced distribution function $G(r)$, calculated by Fourier transformation from the $S(Q)$ data in Fig. 1, for the amorphous Ge–Sb–S–Te system. The curves are shifted vertically for clarity.

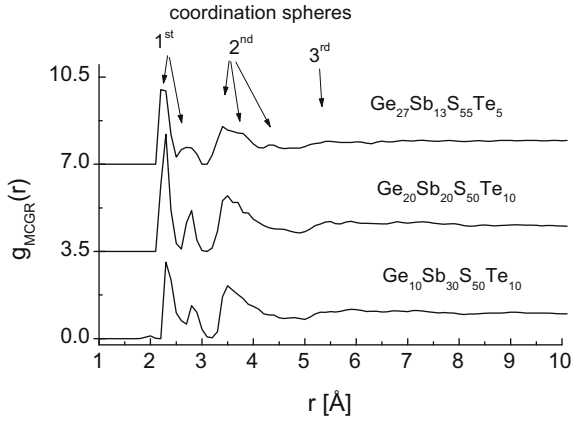

Fig. 3. Atomic pair correlation function $g_{MCGR}(r)$, calculated by MCGR simulation of the $S(Q)$ data in Fig. 1, for the amorphous Ge–Sb–S–Te system. The curves are shifted vertically for clarity.

is not resolved in the spectra. The subsequent atomic neighbour distances are in good agreement with those indicated in Fig. 2.

3. Calculation of some physical parameters of the synthesized glasses

On the basis of the results obtained from the density and composition measurements, for each glass composition we evaluated the molecular weight (M), packing density, coordination number (Z), number of constraints (N_s), average atomic volume (V_a), compactness (δ), average heat of atomization (H_s), and cohesive energy (CE) values. We calculated these physical parameters using literature data [27–32] for each constituent element, summarized in Table 2. The calculation results are presented in Tables 3–5.

Using the ratio $N*\rho/M$, where N is the Avogadro's number and M is the molecular weight, the packing density of the glasses is calculated, the values of which are given in Table 3. As is seen, the packing density decreases with increasing the amount of Ge atoms at constant amount of Te atoms.

The average atomic volume (V_a) was determined from the density data by the equation,

$$V_a = \frac{1}{\rho}\sum_i x_i A_i, \tag{4}$$

where A_i is the atomic weight of the ith component and x_i is the atomic percentage of the same element. The compactness (δ) of the glassy structure was calculated according to the formula [33]:

$$\delta = \frac{\sum_i (x_i A_i)/\rho_i - \sum_i (x_i A_i)/\rho}{\sum_i (x_i A_i)/\rho}, \tag{5}$$

where x_i, A_i, and ρ_i are the atomic fraction, atomic weight and the atomic density of the ith element of the glass and ρ is the measured density of the glass. The V_a and δ are given also in Table 3.

The average coordination number Z is defined by the expression [34]:

$$Z = 4X_{Ge} + 3X_{Sb} + 2X_S + 2X_{Te}, \tag{6}$$

where X is the molar fraction of the constituent elements. The coordination number Z characterizes the electronic properties of semiconducting materials, and shows the bonding character in the nearest-neighbour region [35]. Determination of Z allows the estimation of the number of constraints N_s, which represents a sum of the radial and angular valence force constraints [36] and for a material with a given coordination number Z it can be calculated by Eq. (7).

Table 2
Literature data of the constituent elements in the synthesized glasses.

Property	Ge	Sb	S	Te
Density (g/cm^3) [27]	5.323	6.697	2.07	6.24
Coordination number [28,29]	4	3	2	2 or 3
Bond energy (kcal/mole) [30]	37.6	30.2	50.9	33.0
Atomic mass (g atom) [27]	72.64	121.76	32.06	127.60
Atomic radius (Å) [27]	1.25	1.45	1.00	1.40
Heat of atomization (kcal/g atom) [31,32]	77.71	62.63	66.10	46
Electronegativity [27]	2.01	2.05	2.58	2.1

Table 3
Elemental composition, molecular weight (M), packing density, average atomic volume (V_a), and compactness (δ) of the synthesized chalcogenide glasses.

Composition, measured by PGAA	M (g mole)	Packing density ($\times 10^{22}$ atom/cm^3)	V_a (cm^3/mole)	δ
$Ge_{9.4}Sb_{29.7}S_{50.2}Te_{10.7}$	72.74	3.55	16.96	−0.01841
$Ge_{19.4}Sb_{19.5}S_{50.6}Te_{10.4}$	67.33	3.53	17.04	−0.04448
$Ge_{25.4}Sb_{13.3}S_{51.1}Te_{10.2}$	64.04	3.52	17.13	−0.07263
$Ge_{19.2}Sb_{19.3}S_{56.1}Te_{5.4}$	62.32	3.63	16.58	−0.03950
$Ge_{25.2}Sb_{13.1}S_{56.4}Te_{5.3}$	59.10	3.61	16.70	−0.06356

Table 4
Coordination number (Z), number of constraints (N_s), cohesive energy (CE), and heat of atomization (H_s) of the synthesized glasses, calculated taking into consideration the two-fold and the possible three-fold coordination of Te atoms.

Glass composition	2-Fold coordinated Te atoms			3-Fold coordinated Te atoms			H_s (kcal/g)
	Z	N_s	CE (eV/atom)	Z	N_s	CE (eV/atom)	
$Ge_{9.4}Sb_{29.7}S_{50.2}Te_{10.7}$	2.48	3.20	1.944	2.59	3.48	1.891	64.01
$Ge_{19.4}Sb_{19.5}S_{50.6}Te_{10.4}$	2.58	3.45	2.028	2.68	3.70	2.013	65.52
$Ge_{25.4}Sb_{13.3}S_{51.1}Te_{10.2}$	2.63	3.58	2.228	2.74	3.85	2.228	66.54
$Ge_{19.2}Sb_{19.3}S_{56.1}Te_{5.4}$	2.58	3.45	2.148	2.63	3.58	2.117	66.57
$Ge_{25.2}Sb_{13.1}S_{56.4}Te_{5..3}$	2.64	3.60	2.207	2.69	3.72	2.204	67.50

Table 5
Bond energy, E_{A-B}, and covalent character, C_c, of the possible heteropolar chemical bonds.

Type of chemical bonds	E_{A-B} (kcal/mole)	C_c (%)
Ge–S	53.50	92.20
Te–S	47.90	94.40
Sb–S	47.63	93.22
Ge–Te	35.47	99.80
Ge–Sb	33.75	99.96
Sb–Te	31.64	99.94

$$N_s = (5/2)Z - 3 \tag{7}$$

Although, in Eqs. (6 and 7) the coordination number of Te is given to be equal to 2, in the literature it has been reported [25] that three-fold coordinated Te atoms are also possible. Despite the fact that the percent of three-fold coordinated Te is supposed to be small (~17%) in the reported ternary Ge–Sb–Te alloys [25], we considered both possible coordination number of Te atoms, i.e. 2 and 3, in the calculations of Z and N_s values for our quaternary Ge–Sb-(S,Te) system. As it is seen from Table 4, the calculated values are close but in the case of two-fold coordinated Te atoms, the Z and N_s values remain constant with increasing the Te content, while for the three-fold coordination of Te the Z and N_s values increase with increasing the Te atoms.

Based on the chemical bond approach, where the bond energies are assumed to be additive, we estimated the cohesive energy (CE) by summarizing the bond energies over all the possible chemical bonds expected in the glasses. The bonds are formed in strict sequence decreasing their bond energy until all the valences of the atoms are saturated [37]. According to the Pauling relationships [38] the covalent bond energy E_{A-B} between atoms A and B and the degree of covalency, C_c, of these bonds can be derived from the expressions:

$$E_{A\text{-}B} = (E_{A-A}E_{B\text{-}B})^{1/2} + 30(x_A - x_B)^2 \quad \text{and}$$
$$C_c = 100\exp\left[-(x_A - x_B)^2/4\right], \tag{8}$$

where E_{A-A} and E_{B-B} are the single-bond energies and x_A and x_B are the electronegativities of atoms A and B, respectively, and they are taken from Table 2. The calculated values of these parameters are presented in Table 5. According to the chemical bond ordering, the covalent bond energy E_{A-B} decreases with increasing the degree of covalency C_c. Determining the bond energies (E_{A-B}) and the percent of each possible chemical bond in the composition, and taking into account the chemical bond ordering, the cohesive energy (CE) values were calculated (Table 4). The difference of the CE values for 2- and 3-fold coordinated Te atoms is negligibly small.

In the case of binary semiconductor material, formed from atoms A and B, for room temperature and atmospheric pressure conditions the heat of atomization (H_s) can be determined as:

$$H_s(\text{A-B}) = \Delta H + 1/2\left(H_s^A + H_s^B\right), \tag{9}$$

where ΔH is the heat of formation and H_s^A and H_s^B are the heat of atomization of atom A and B, respectively, and correspond to the average nonpolar bond energy of A–A and B–B chemical bonds [39]. In most cases the heat of formation of chalcogenide glasses is unknown. Even for those few glasses, for which the heat of formation ΔH is known, its value does not exceed 10% of the heat of atomization and, therefore, it can be neglected [40,41] and H_s(A–B) can be determined as:

$$H_s(\text{A-B}) = 1/2\left(H_s^A + H_s^B\right). \tag{10}$$

For a ternary system $A_\alpha B_\beta C_\gamma$, the average heat of atomization can be calculated as [42]:

$$H_s = \left(\alpha H_s^A + \beta H_s^B + \gamma H_s^C\right)/(\alpha + \beta + \gamma). \tag{11}$$

For a multi-component semiconductor system the same consideration can be applied [42]. Therefore, we calculated the average heat of atomization H_s of the glasses synthesized by us using the H_s values of constituent elements given in Table 2. The results are presented also in Table 4.

4. Discussion

The neutron diffraction measurements have revealed that the synthesized glasses are fully amorphous, as evidenced from the lack of characteristic Bragg peaks of a crystalline phase and the wavy character of the curves of the structural factor $S(Q)$ (Fig. 1). At first glance, the curves in Fig. 1 are similar to each other suggesting similarity of the glass network structure. However, in the fine details slight changes may be observed. The sharpening of the first sharp peak in Fig. 1 is an evidence for medium range ordering in the structure of these glasses. As was mentioned above, the distinct peak, appeared at ~2.3 Å in Fig. 3, is associated with the Ge–S first neighbour distance, while the distinct peak at ~2.8 Å is associated with the Sb–Te first neighbour distance [24–26]. As it was also mentioned, the Ge–Ge first neighbour distance, expected around 2.4 Å [25,26], is not resolved in the spectra. In order to get more information on the local structure, the partial atomic correlation functions should be calculated by computer modelling with RMC simulation, which is beyond the scope of this paper.

Any changes in the glass density are related to the change in the atomic weight and volume of the elements constituting the system. Since the atomic radiuses of Ge and Sb are close to each other and the atomic mass of Ge is much smaller than that of the Sb atom (Table 2), changing the composition by increasing Ge content at the expense of Sb content results in a decrease of glass density (Table 1). Due to the stronger influence of glass density than the effect of atomic size, the packing density also decreases by increasing the Ge content (Table 3). Highly cross-linked network with a three-dimensional organization yields low packing density, which contributes to a further decrease of the packing density of these glasses. For our glassy system, by substituting Te for S atoms and increasing the amount of Te atoms, the glass density increases

and the packing density decreases due to the much larger mass and atomic radius of the Te atoms.

The compactness (δ) is a measure of the normalized change of the average atomic volume due to chemical interactions of the elements forming the network of a given glass and, therefore, is associated with the free volume and flexibility of this network [17]. The compactness can have negative values and implicitly the glasses possess larger free volume and flexibility. Consequently, δ is more sensitive to changes in the structure of the glass network than to the average atomic volume. The glasses investigated here have the highest compactness at the smallest amount of Ge and at a constant amount of Te or at the smaller amount of Te and at a constant amount of Ge (Table 3). It is evident that both V_a and δ values are affected by the interaction between the constituent elements and the connectivity of a glassy network. The stability of the network depends on the atomic arrangements; the stronger the chemical bonds and the shorter the bond length, the smaller the average atomic volume and the larger the compactness of the network.

On the basis of the average number of bonds/atom, Z, and the average number of valence bonding stretching and bending constraints/atom, N_s, the chalcogenide glasses can be organized into three different categories according to the constrain theory [43]: (i) floppy, or under-coordinated glasses with $Z < 2.4$ and $N_s < 3$; (ii) optimally-coordinated or ideal glasses with $Z = 2.4$ and $N_s = 3$; (iii) stressed-rigid and over-coordinated glasses with $Z > 2.4$ and $N_s > 3$. In accordance with that, the glassy compositions studied by us are over-coordinated and stressed-rigid, as the values of Z are larger than 2.4 and the N_s values are larger than 3 (Table 4). In general, glasses with N_s either being larger or smaller than 3, have a highly defective structure. The possible existence of three-fold coordinated Te atoms will make these glasses even more over-coordinated and stressed-rigid.

From the bonding energy values (E_{A-B} in Table 5) it follows that Ge–S bonds with the highest possible energy are expected to be formed first, followed by the Te–S and Sb–S bonds till saturation of all available valence of S and Te is achieved. There are still some unsaturated bonds of Sb, which must be bonded through formation of homopolar Sb–Sb bonds, being defects in the glass structure. The cohesive energy CE values have a tendency to increase with increasing the Ge and decreasing the Te contents (Table 4). It should be mentioned that the chemical bonds approach neglects dangling bonds and other valence defects, as well as van der Walls interactions. We suggest that consideration of these factors would lead to a further increase of the CE values by formation of much weaker links than regular covalent bonds.

In the case when the content of Te is kept constant and the content of Ge gradually increases, the amount of $GeS_{4/2}$ tetrahedral unit increases at the expense of $SbS_{3/2}$ pyramidal units, replacing the weaker Sb–S bonds with the stronger Ge–S ones. This in turn increases the cohesive energy CE as observed (Table 4). In the opposite case when the content of Ge is kept constant and the content of Te increases, the two-fold coordinated Te atoms replace S atoms in the $GeS_{4/2}$ tetrahedral and $SbS_{3/2}$ pyramidal units, and form $[SbS_{3-x}Te_x]$ mixed pyramidal and $[GeS_{4-x}Te_x]$ mixed tetrahedral units. As a consequence, the replacement of the stronger Ge–S and Sb–S with the weaker Ge–Te and Sb–Te bonds causes lowering of the cohesive energy. Supposing that three-fold coordination of Te atoms exists, the cohesive energy for all the compositions studied becomes smaller as it can be seen from the comparison of the CE values in Table 4. Assuming the possibility that the Te atoms in the glasses are with three-fold coordination means that the formed glassy structure has to be even more defective and unstable.

The average heat of atomization (H_s) is also a measure of the cohesive energy and it represents the relative bond strength, which in turn is correlated with the energy gap of isostructural semiconductors. According to Ref. [44], for overconstrained materials with higher connectivity ($3 \leqslant Z \leqslant 4$) the energy bandgap depends much more strongly on H_s than for glasses with lower connectivity ($2 \leqslant Z \leqslant 3$). As is seen from Table 4, these glasses are with lower connectivity ($2 < Z < 3$) and the parameter H_s/Z is almost constant independently on composition. Therefore, the average heat of atomization H_s would have a negligible effect on the bandgap energy values.

The results in Table 5 point out that these glasses possess predominantly covalent bonds, supported by the fact that the constituent elements in the investigated glasses have close values of electronegativity (Table 2). It is reasonable to suggest that the covalent network of these glasses will be the decisive factor determining their various properties.

5. Conclusions

New amorphous quaternary telluride glassy materials have been synthesized with composition of $Ge_xSb_{40-x}S_{50}Te_{10}$ ($x = 10$, 20 and 27 at.%) and $Ge_xSb_{40-x}S_{55}Te_5$ ($x = 20$ and 27 at.%). It has been shown that in the amorphous glasses the 1st coordination sphere is related to the Ge–S and Sb–Te first neighbour distances of 2.3 and 2.8 Å, respectively. From the measured composition and density of these glasses the physical parameters, namely packing density, average atomic volume, compactness, coordination number, number of constrains, cohesive energy, and heat of atomization have been evaluated. These parameters are well-correlated with the network-terminating role of Ge and/or Te atoms.

Acknowledgements

The authors gratefully acknowledge the partial support of this work by EU 7FP: Grant Agreement No. 226507-NMI3.

References

[1] A.B. Seddon, M.J. Laine, J. Non-Cryst. Solids 213&214 (1997) 168.
[2] K. Abe, H. Takebe, K. Morinaga, J. Non-Cryst. Solids 212 (1997) 143.
[3] D.R. Simons, A.J. Faber, H. DeWaal, J. Non-Cryst. Solids 185 (1995) 283.
[4] R. Zallen, The Physics of Amorphous Solids, Wiley, New York, 1983.
[5] Z. Ling, H. Ling, Z. Cheng Shan, J. Non-Cryst. Solids 184 (1995) 1.
[6] A. Znobrik, J. Stetzif, I. Kavich, V. Osipenko, I. Zachko, N. Balota, O. Jakivchuk, Ukr. Phys. J. 26 (1981) 212.
[7] M. Cable, J.M. Parker (Eds.), High-performance Glasses, Blackie, Glasgow, 1992.
[8] S.R. Elliott, Physics of Amorphous Materials, Longman, 1990.
[9] V. Pamukchieva, A. Szekeres, Opt. Mater. 30 (2008) 1088.
[10] V.S. Shiryaev, J.-L. Adam, X.H. Zhang, C. Boussard-Plerdel, J. Lucas, M.F. Churbanov, J. Non-Cryst. Solids 336 (2004) 113.
[11] K. Michel, B. Bureau, C. Pouvreau, J.C. Sangleboeuf, C. Boussard-Plédel, T. Jouan, T. Rouxel, J.-L. Adam, K. Staubmann, H. Steinner, T. Baumann, A. Katzir, J. Bayona, W. Konz, J. Non-Cryst. Solids 326&327 (2003) 434.
[12] J. Keirsse, C. Boussard-Plédel, O. Loreal, O. Sire, B. Bureau, B. Turlin, P. Leroyer, J. Lucas, J. Non-Cryst. Solids 326&327 (2003) 430.
[13] D. Le Coq, C. Boussard-Plédel, G. Fonteneau, T. Pain, B. Bureau, J.L. Adam, Mater. Res. Bull. 38 (2003) 174.
[14] M. Dongol, M.M. Hafiz, M. Abou-Zied, A.F. Elhady, Appl. Surf. Sci. 185 (2001) 1.
[15] V. Pamukchieva, A. Szekeres, K. Todorova, Proc. SPIE 5581 (2004) 608.
[16] V. Pamukchieva, A. Szekeres, J. Optoelectron. & Adv. Mater. 7 (2005) 1277.
[17] L. Tichy, H. Ticha, Mater. Lett. 21 (1994) 313.
[18] L. Tichy, H. Ticha, J. Non-Cryst. Solids 189 (1995) 141.
[19] J.P. Deneufville, H.K. Rockstad, in: J. Stuke, W. Brenig (Eds.), Amorphous Liquid Semiconductors, Taylor&Francis, London, 1974.
[20] E. Sváb, Gy. Mészáros, F. Deák, Mater. Sci. Forum 228 (1996) 247. http://www.bnc.hu/.
[21] E. Sváb, Gy. Mészáros, G. Konczos, S.N. Ishmaev, S.L. Isakov, A.A. Chernyshov, J. Non-Cryst. Solids 104 (1988) 291.
[22] L. Pusztai, R.L. McGreevy, Physica B 234 (1997) 357.
[23] R.L. McGreevy, L. Pusztai, Mol. Simul. 1 (1988) 359.
[24] F. Sava, A. Anghel, I. Kaban, W. Hoyer, M. Popescu, Chalcogenide Lett. 2 (2005) 49.
[25] D.A. Baker, M.A. Paesler, G. Lucovsky, P.C. Taylor, J. Non-Cryst. Solids 252 (2006) 1621.
[26] P. Jóvári, I. Kaban, J. Steiner, B. Beuneu, A. Schöps, A. Webb, J. Phys.: Condens. Mater. 19 (2007) 335212.
[27] http://www.knovel.com/web/portal/periodic_table.
[28] V. Pamukchieva, E. Savova, Thin Solid Films 347 (1999) 226.

[29] M. Fadel, Vacuum 48 (1997) 73.
[30] J. Bicerano, S.R. Ovshinsky, Chemical Bonding and the Nature of Glass Structure, in: V.H. Smith Jr., H.F. Schaefer, K.D. Morokuma (Eds.), Appl. Quantum Chem., Reidel Publishing Company, Holland, 1986.
[31] Ambika, P.B. Barman, J. Ovonic Res. 3 (2007) 21.
[32] http://www.periodni.com/en/index.html.
[33] O.I. Shpotyuk, T. Kavetskiy, A.P. Kovalskiy, V. Pamukchieva, Proc. SPIE 4415 (2001) 278.
[34] N. Yamaguchi, Philos. Mag. 51 (1985) 651.
[35] A.F. Ioffe, A.R. Regel, Prog. Semicond. 4 (1960) 239.
[36] S.C. Agarwal, M.A. Paesler, D.A. Baker, P.C. Taylor, G. Lucovsky, A. Edwards, Pramana J. Phys., Indian Acad. Sci. 70 (2008) 245.
[37] B. Jozef, O. Stanford, S. Mahadevan, A. Gridhar, A.K. Singh, J. Non-Cryst. Solids 74 (1985) 75.
[38] L. Pauling, The Nature of the Chemical Bond, Cornell University Press, Ithaca, NY, 1960.
[39] L. Pauling, J. Phys. Chem. 58 (1954) 662.
[40] S.S. Fouad, Vacuum 52 (1999) 505.
[41] S.S. Fouad, A.H. Ammar, M. Abo-Ghazala, Physica B 229 (1997) 249.
[42] V. Sadagopan, H.C. Gotos, Solid-State Electron. 8 (1965) 529.
[43] J.C. Phillips, M.F. Thorpe, Solid State Commun. 53 (1985) 699.
[44] M. Kastner, Phys. Rev. Lett. 28 (1972) 355.